Accepted version of IEEE-copyrighted article. The original version of this article is available at: https://ieeexplore.ieee.org/document/9793579.
DOI: 10.1109/TPEL.2022.3181495

Continuously-Adjustable Modular Bidirectional Switched-Capacitor DC-DC Converter

Shouheng Han, *Student Member*, *IEEE*, Yijie Wang, *Senior Member*, *IEEE*, Zhenli Xie, Yueshi Guan, *Senior Member, IEEE,* J. Marcos Alonso, *Fellow, IEEE* and Dianguo Xu, *Fellow, IEEE*

***Abstract*—This letter proposes a switched capacitor (SC) based continuously-adjustable modular bidirectional DC-DC converter. The structure of the proposed converter consists of 3 types of modules, series-parallel switched capacitor converter (SCC) module, regulating module, and resonant switched capacitor converters (RSCC) module. A basic configuration of 3 modules working in buck operating mode is analyzed in detail. The boost mode operation is symmetrical to the buck mode. The regulation module provides all regulation capability, the other two modules operate at fixed duty cycle and provide the main conversion ratio. A prototype of the basic configuration was built to verify the theory. The peak efficiency of the prototype is 97.15%.**

***Index Terms*—Bidirectional power flow, buck-boost, DC-DC converters, modular design, switched capacitor circuits.**

I. Introduction

As new energy accounts for a gradual increase in overall energy consumption, the demand for energy storage is also growing rapidly in order to maintain a stable operation of the power grid. Research on the topology of energy bidirectional transmission has also received more attention. Due to the working characteristics of switched capacitor topology, it can realize bidirectional transfer of energy easily.

Since the switched capacitor topology does not contain a transformer, which occupies most of the weight and volume of the converter, it can form a higher power density converter [1, 2]. In addition, it also has the advantages of simple structure and easy modularization and integration.

To overcome the transient high current in SCC, RSCC have been proposed [3-13]. The RSCC topology incorporates an inductor to form a resonant circuit to smooth the switching current. Based on this principle, many RSCC topologies have been improved. A switched-tank converter using GaN devices is proposed in [7]. The peak efficiency is 98.55% and the conversion ratio is fixed. Reference [8] presents a 4 to 1 fixed ratio RSCC converter. The efficiency of this prototype is over 97% at rated operating conditions.

Through proper driving circuit and control loop design, soft switching can be realized to improve the overall efficiency of the SCC. However, most RSCC are topologies with fixed conversion ratios, which limits the wide application of RSCCs. Some studies have given some methods to adjust the output of RSCC. A resonant switched capacitor with high efficiency over a wide and continuous conversion ratio range is introduced in [3]. Reference [4, 5] dim the resonant current of the inductor in an RSC-based LED driver with variable inductor control method. Some articles add conditioning units before or after the SCC stage to tune the output. Although this topology is simple and easy to implement, the two-stage structure will inevitably have an impact on the efficiency of the entire converter.

Reference [6] proposes a non-isolated SC-based multiport converter for stand-alone photovoltaic systems. Due to the feature that energy can flow in both directions in the switched capacitor topology, the switched capacitor [6] acts as a bridge between the power generation terminal, the battery terminal, and the load terminal. A 100-kW switched tank converter (STC) using SiC MOSFETs for transportation power electronic systems is presented in [9]. This bidirectional SCC is designed for 300-600 V voltage conversion. The converter is composed of multiple RSCC modules in parallel, but the filter capacitors on the series connection side may have different capacitances, which will cause power recirculation and reduce efficiency. Reference [10] proposes a non-isolated bidirectional DC–DC converter based on coupled inductors and switched capacitor. However, due to the introduction of coupled inductors, the design and control of the converter are relatively complicated.

This letter proposed a switched capacitor based continuously adjustable modular bidirectional converter, which can easily be extended to higher conversion ratio. The control method of the converter is relatively simple, and the output can be continuously adjusted. The proposed topology configuration and operating principle are expounded in Section II. The experiment conditions and prototype parameters are provided in Section III. A photo of the protype is given with thermal image. Experiment waveforms of all modules are provided and evaluated. The peak efficiencies are 97.15% at boost mode and 97.11% at buck mode, while the efficiencies at full load are 95.99% and 95.92% respectively. A conclusion section is given in the last part of this letter.

II. Proposed Topology

A. Configuration

The proposed converter can be modularized as shown in the schematic of Fig. 1. It consists of three modules, input SCC module, regulating module, and RSCC module. The number of modules is selected according to the needs of the converter. When the converter needs better regulation performance, more regulation modules are added. When a higher transformation ratio is required, more RSCC modules are added.

In common input series output parallel (ISOP) converters, the input capacitors of different modules need to maintain a high consistency to ensure that the input voltages of each module are the same. The input SCC module is a series-parallel SCC topology. Because of the characteristics of switched capacitors, the input voltage is evenly distributed among the different modules, regardless of the input capacitance values of them. The input capacitor of the regulating module is relatively small compared to that of the RSCC module, since more power is transfer through RSCC module.

The simplest form of the proposed topology is given in Fig.2. It consists of 1 SCC module, 1 regulating module, and 1 voltage doubler (VD) module. The switches of the VD module operate with a fixed duty cycle of 0.5. The voltage conversion ratio is controlled by adjusting the duty cycle of the regulating module. Taking buck mode as an example,

$$V_{H} = V_{b} + V_{scc} \tag{1}$$

where V_H is the input voltage, V_b is the voltage of C_b, V_{scc} is the voltage of C_{scc}.

$$V_{out} = D \bullet V_{b} \tag{2}$$

where D is the duty cycle of the regulating module.

$$V_{out} = \frac{1}{m} V_{scc} \tag{3}$$

where m is the conversion ratio of VD module.

According to (2), (3),

$$V_{H} = \frac{1}{D} V_{out} + m V_{out} = (m + \frac{1}{D}) V_{out} \tag{4}$$

$$M = \frac{V_{out}}{V_{H}} = \frac{V_{L}}{V_{H}} = \frac{D}{mD+1} \tag{5}$$

where V_L is the output voltage.

The voltage conversion ratio of the basic topology is shown in Fig. 3. The conversion ratio of the VD module increases in multiples according to the law of 2^n.

B. Operating Principle

The output is adjusted through varying the duty cycle (D) of the regulating module. Fig. 4 shows the timing diagram of all driving signals. Q_{b1} and Q_{b3} use the same driving signal. The shaded part in the figure is the adjustable range of Q_{b1}, Q_{b3} and Q_{b2}, i.e., the D of regulating module. The topology in Fig. 2 cycle works in 6 states, both in buck and boost mode, when D is 0.6. The switching states of the proposed basic topology in buck mode are shown in Fig. 5. According to the module to which it belongs, the current flow direction is highlighted in three colors.

In the first State, Q_{H1}, Q_{H2}, Q_{b2}, Q_1 and Q_3 are off. Q_{b1}, Q_{b3}, Q_2 and Q_4 are on. The energy is transfer from C_b and L_b in the regulating module to the output. In SCC module, it is from C_r and L_{scc}. At second State, Q_{H1} and Q_{H2} are off. No energy is transferred to C_b and C_{scc}. Q_{b1} and Q_{b3}, are off and Q_{b2} is on. The regulating module transfer energy from L_b to C_L. Q_2 and Q_4 are on, Q_1 and Q_3 are off. The SCC module transfer energy from C_r and L_{scc} to C_L. At third State, switch Q_{H1} and Q_{H2} turn on. The input capacitors of parallel modules C_b and C_{scc} are charged in series, the voltage distribution is based on the voltage conversion ratio of the regulating module and the VD module. The other switches keep their working state same. At fourth State, Q_{H1} and Q_{H2} turn off. The switch states of other switches remain unchanged until t_4. For the fifth State, Q_{b1} and Q_{b3} turn

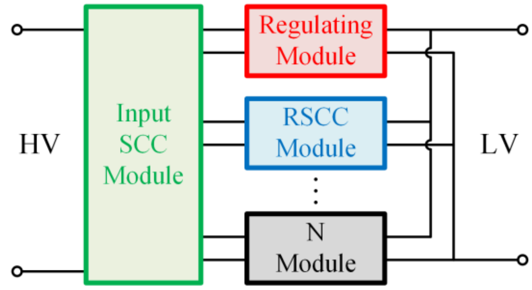

Fig. 1. The structure of the proposed topology

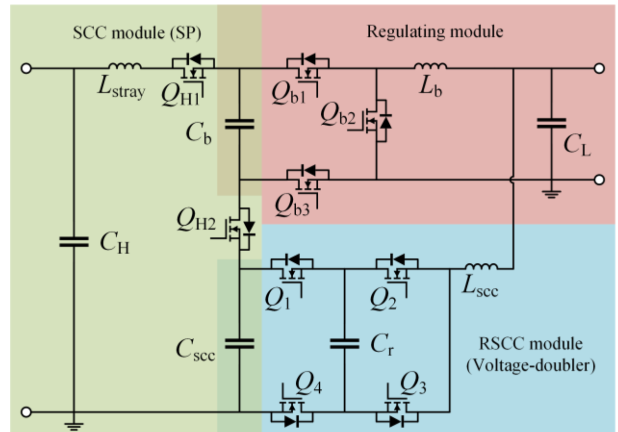

Fig. 2. Basic topology of proposed converter.

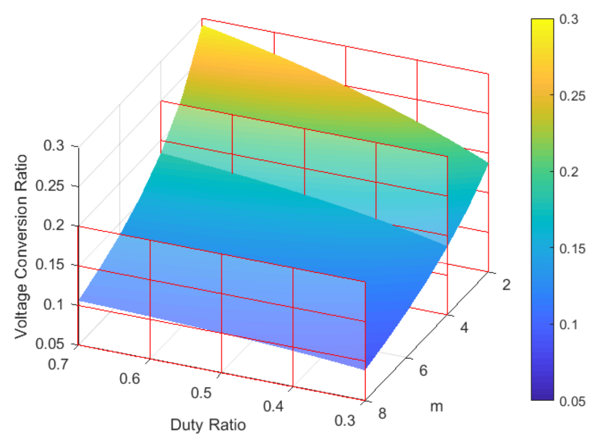

Fig. 3 Voltage conversion ratio of basic topology

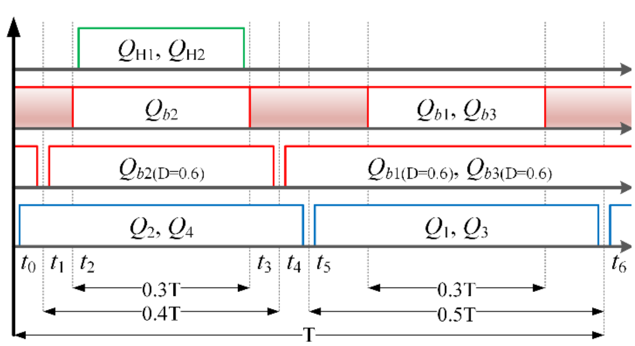
Fig. 4 Timing diagram of all switches driving signal.

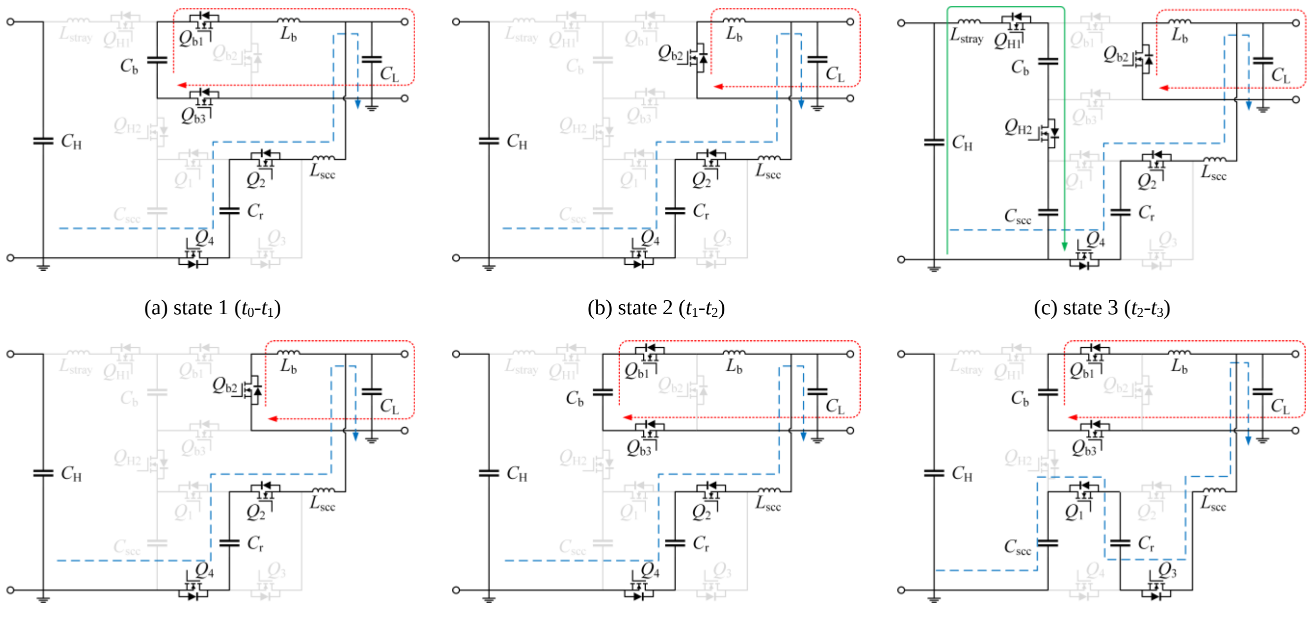

(a) state 1 (t_0-t_1) (b) state 2 (t_1-t_2) (c) state 3 (t_2-t_3)

(d) state 4 (t_3-t_4) (e) state 5 (t_4-t_5) (f) state 6 (t_5-t_6)

Fig. 5 Switching states of the basic topology operating at D=0.6 (Buck-mode) (a) state 1 (t_0-t_1). (b) state 2 (t_1-t_2). (c) state 3 (t_2-t_3). (d) state 4 (t_3-t_4). (e) state 5 (t_4-t_5). (f) state 6 (t_5-t_6).

on, Q_{b2} turn off at t_4. Q_{H1} and Q_{H2} stay off. The SCC module remains unchanged. At the last state, Q_{H1} and Q_{H2} remain off. In regulating module, C_b charges L_b and C_L in series. In the meantime, Q_1 and Q_3 turn on, Q_2 and Q_4 turn off. In the VD module, C_{scc} charges C_r and C_L in series. The duty cycles of Q_{H1}, Q_{H2}, Q_1, Q_2, Q_3 and Q_4 are fixed. Only the duty cycle of the switches in the regulating module needs to be adjusted according to the required output voltage.

III. Experimental Results

A prototype has been built to verify the theoretical analysis. The parameters of the prototype are listed in Table I.

The step-down experiment is taken with 48 V input and 12 V output. The rated output power and rated output current are 200W and 16.67A respectively. All the switches are working with 100 kHz switching frequency. The experimental conditions of boost

TABLE I
Parameters Of The Components In Prototype

Components	Voltage Stress	Values and Main Parameters	Manufacturer and Part No.
C_r	<0.5V_H	26uF	muRata
L_b	/	10uH	BC
L_{scc}	/	100nH	ABRACON
Q_{b1}	V_H	V_{DS}=60V, I_D=20A, $R_{DS(ON)MAX}$=6.7mΩ	BSZ067N06LS3 G
Q_{H1}, Q_{H2}, Q_{b2}, Q_{b3}	0.5V_H	V_{DS}=40V, I_D=40A, $R_{DS(ON)MAX}$=4mΩ	BSZ040N04LS G
Q_1, Q_2, Q_3, Q_4	0.25V_H+ΔC_r	V_{DS}=40V, I_D=40A, $R_{DS(ON)MAX}$=4mΩ	BSZ040N04LS G

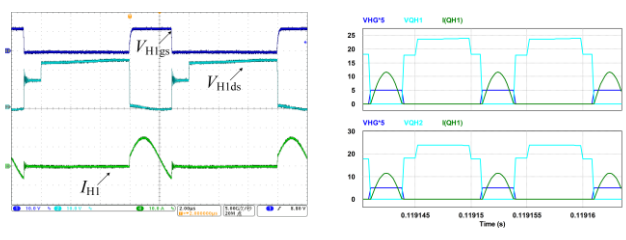

Fig. 6. Experimental and simulation waveforms of input SCC module

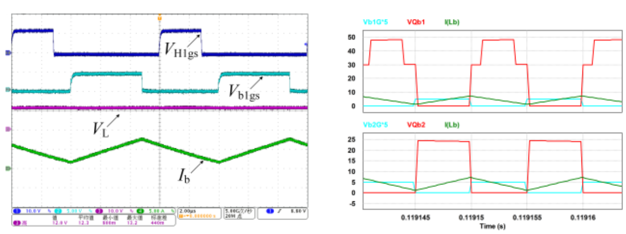

Fig. 7 Experimental and simulation waveforms of regulating module

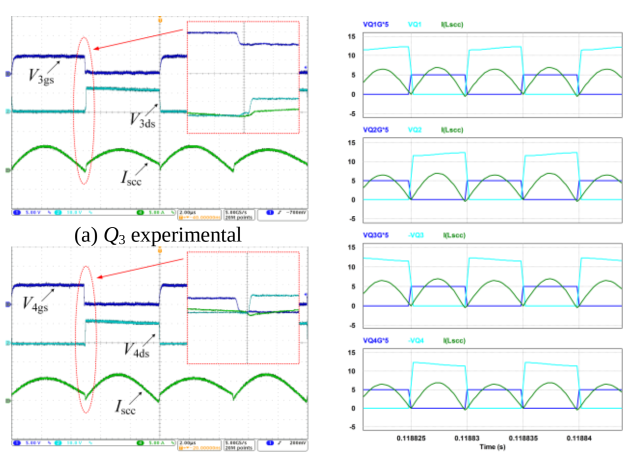

(a) Q_3 experimental

(b) Q_4 experimental (c) Q_1-Q_4 simulation

Fig. 8 Experimental and simulation waveforms of VD module

TABLE II
COMPARISON OF THIS WORK AND PRIOR ARTS

	Power density at full load	Efficiency	No. of switches	PCB parameters	Voltage conversion ratio
Switched-Tank Converter [7]	1000W/in^3 at 600W	98.71% peak 97% full load	16 switch	10 layer 2 oz	V_{in}=54V V_{out}=8.7V 6:1 unregulated
Cascaded Resonant Converter [8]	2500W/in^3 at 720W	99% peak 97.2% full load	16 switch	4 layer 2 oz	V_{in}=48V V_{out}=12V 4:1 unregulated
Multiport Converter [6]	60W/in^3 estimated at 150W (Components are loosely placed)	94% full load	6 switch 4 diode	Not mentioned	V_{in}=30V V_{out}=28V, V_{bat}=12-16V regulated
This work	117.1W/in^3 at 200W (Components are loosely placed)	97.15% peak 95.92% full load	9 switch	4 layer 1 oz	V_{in}=48V V_{out}=9-14V regulated

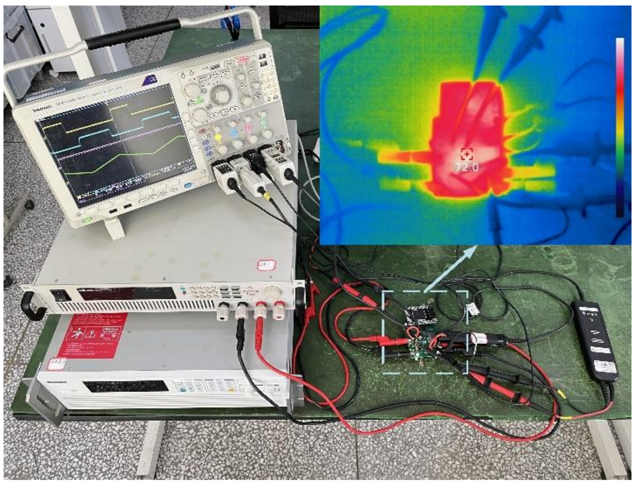

Fig. 9 Photo of the prototype

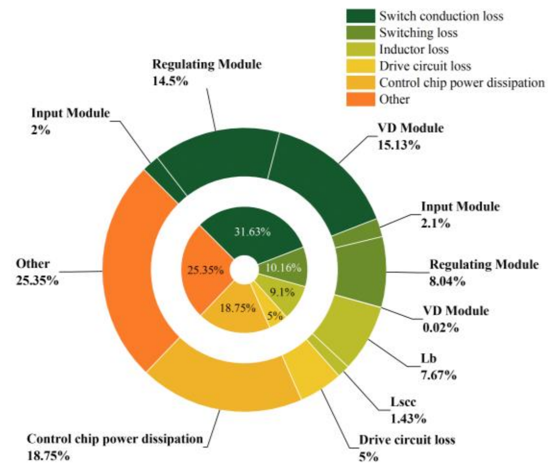

Fig. 11 Loss breakdown

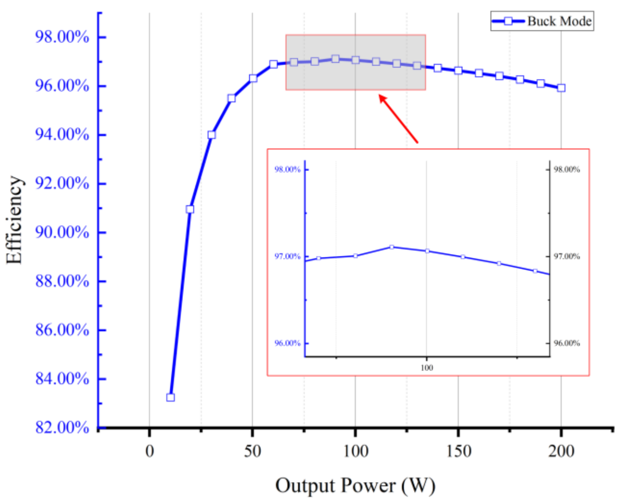

Fig. 10 Efficiency of Buck Mode at different Output Power

mode are a clone of buck mode. According to the state analysis, the switching frequency of all modules must be the same. If the switching frequency is increased, the volume of passive components will be further reduced. The duty cycle of SP module is chosen to be 0.3. Therefore, the resonant frequency should be 166 kHz to achieve soft switching. In the VD module the duty cycle is 0.5, so 100 kHz resonant frequency is applied.

The experimental and simulation waveforms of the input SCC module are given in Fig. 6. Simulated and experimental waveforms for the same component are represented by the same color. The left figure is the experimental waveform of Q_{H1}. The upper part of the figure on the right is the simulated waveform of Q_{H1}. The bottom half is the simulated waveform of Q_{H2}.

The stray inductance is measured through an impedance analyzer (E4990A by Keysight Tech.). The parasitic inductance measured by the impedance analyzer is from ten nH to several tens of nH, which is not 100% accurate. The input capacitance of the module can be designed according to this range, and the experimental results verify that the estimated range is close. However, it can be seen from Fig. 6 that the two switches Q_{H1} and Q_{H2} do not achieve ZCS, and V_{H1ds} oscillates when Q_{H1} is turned off. The perfect soft-switching of SP module will be studied in a future work.

The experimental and simulated waveforms of the input module are different between t_1-t_2. When Q_{b1} is turned off, no current can charge the parasitic capacitance of Q_{b3}, so the lower end of C_b is still at ground potential, the voltage across Q_{b1} is still about 0.5V_H. The switches in the simulation are ideal switches, so the waveforms are different.

Fig. 7 and Fig. 8 are the experimental and simulation waveforms of the regulating and VD modules. All switches of voltage-doubler module are achieving soft switching. Waveforms of the same component are represented by the same color. The left figure of Fig. 7 is the experimental waveform of Q_{b1}. The upper part of the figure on the right side of Fig. 7 is the simulated waveform of Q_{b1}.

The bottom half is the simulated waveform of Q_{b2}. The red simulation waveforms are V_{DS} of the switches.

The boost mode operation is symmetrical with buck mode operation. At the same duty cycle, the waveforms of all components are similar. Therefore, no further analysis will be made.

Fig. 9 shows the photo of experimental set up. The upper right corner shows the thermal image of the prototype operating at maximum power for 30 minutes at room temperature. The maximum temperature point is 72 ℃ . The efficiency of buck mode at different output power is given in Fig. 10. The output power was adjusted by varying the output load value. The peak efficiencies of boost mode and buck mode are 97.15% and 97.11%. The efficiencies at full load are 95.99% and 95.92% respectively. The efficiency is almost the same at buck and boost mode.

A loss breakdown, when the converter is operating at full load, is introduced in Fig. 11. The regulating module suffers the worst loss due to hard switching in this part. The main part of 'Other' in the loss breakdown is the conduction loss of the PCB. The PCB used in the prototype is a four-layer version with an outer copper thickness of 1oz, and the main power circuit is placed on the top layer. Therefore, using a PCB with thicker copper tracks and more layers can effectively reduce losses.

A comparison between this work and the similar switched-capacitor based resonant converters is given in Table II. The same conversion ratio is achieved here using fewer switching elements compared to the prior art. Due to the needs of testing, the components in the prototype are not closely arranged. If a good layout is carried out, the power density will be greatly improved. In addition, this work has higher efficiency compared to other converters with regulation capability.

IV. CONCLUSION

A switched capacitor based continuously adjustable modular bidirectional DC-DC converter is proposed in this letter. The structure of the proposed converter consists of 3 types of modules: series-parallel switched capacitor converter module, regulating module, and voltage doubler module. The converter can be easily extended to higher conversion ratios due to the modular design of the topology. The control method of the converter is relatively simple, and the output can be continuously adjusted. The efficiency of the converter is above 95.95% in most of the operating range.

REFERENCES

[1] Y. Ye, G. Zhang, X. Wang, Y. Yi, and K. W. E. Cheng, "Self-Balanced Switched-Capacitor Thirteen-Level Inverters With Reduced Capacitors Count," *IEEE Transactions on Industrial Electronics,* vol. 69, no. 1, pp. 1070-1076, 2022.

[2] N. Sandeep, J. S. M. Ali, U. R. Yaragatti, and K. Vijayakumar, "Switched-Capacitor-Based Quadruple-Boost Nine-Level Inverter," *IEEE Transactions on Power Electronics,* vol. 34, no. 8, pp. 7147-7150, 2019.

[3] A. Cervera, M. Evzelman, M. M. Peretz, and S. Ben-Yaakov, "A High-Efficiency Resonant Switched Capacitor Converter With Continuous Conversion Ratio," (in English), *Ieee Transactions on Power Electronics,* vol. 30, no. 3, pp. 1373-1382, Mar 2015.

[4] M. Martins, M. S. Perdigao, A. M. S. Mendes, R. A. Pinto, and J. M. Alonso, "Analysis, Design, and Experimentation of a Dimmable Resonant-Switched-Capacitor LED Driver With Variable Inductor Control," *IEEE Transactions on Power Electronics,* vol. 32, no. 4, pp. 3051-3062, Apr 2017.

[5] G. Martinez, J. M. Alonso, and R. Osorio, "Analysis and Design of a Unidirectional Resonant Switched-Capacitor Step-Up Converter for OLED Lamp Driving Based on Variable Inductor," *IEEE Journal of Emerging and Selected Topics in Power Electronics,* vol. 6, no. 3, pp. 1106-1115, Sep 2018.

[6] M. Uno and K. Sugiyama, "Switched Capacitor Converter Based Multiport Converter Integrating Bidirectional PWM and Series-Resonant Converters for Standalone Photovoltaic Systems," *IEEE Transactions on Power Electronics,* vol. 34, no. 2, pp. 1394-1406, 2019.

[7] X. Lyu, Y. Li, N. Ren, C. Nan, D. Cao, and S. Jiang, "Optimization of High-Density and High-Efficiency Switched-Tank Converter for Data Center Applications," *IEEE Transactions on Industrial Electronics,* vol. 67, no. 2, pp. 1626-1637, 2020.

[8] Z. Ye, Y. Lei, and R. C. N. Pilawa-Podgurski, "The Cascaded Resonant Converter: A Hybrid Switched-Capacitor Topology With High Power Density and Efficiency," *IEEE Transactions on Power Electronics,* vol. 35, no. 5, pp. 4946-4958, 2020.

[9] Z. Ni, Y. Li, C. Liu, M. Wei, and D. Cao, "A 100-kW SiC Switched Tank Converter for Transportation Electrification," *IEEE Transactions on Power Electronics,* vol. 35, no. 6, pp. 5770-5784, 2020.

[10] R. Hu, J. Zeng, J. Liu, and K. W. E. Cheng, "A Nonisolated Bidirectional DC–DC Converter With High Voltage Conversion Ratio Based on Coupled Inductor and Switched Capacitor," *IEEE Transactions on Industrial Electronics,* vol. 68, no. 2, pp. 1155-1165, 2021.

[11] K. Li, Y. Hu, and A. Ioinovici, "Generation of the Large DC Gain Step-Up Nonisolated Converters in Conjunction With Renewable Energy Sources Starting From a Proposed Geometric Structure," *IEEE Transactions on Power Electronics,* vol. 32, no. 7, pp. 5323-5340, 2017.

[12] T. Modeer, N. Pallo, T. Foulkes, C. B. Barth, and R. C. N. Pilawa-Podgurski, "Design of a GaN-Based Interleaved Nine-Level Flying Capacitor Multilevel Inverter for Electric Aircraft Applications," *IEEE Transactions on Power Electronics,* vol. 35, no. 11, pp. 12153-12165, 2020.

[13] J. Baek *et al.*, "Vertical Stacked LEGO-PoL CPU Voltage Regulator," *IEEE Transactions on Power Electronics,* vol. 37, no. 6, pp. 6305-6322, 2022.